IJMOT

INTERNATIONAL JOURNAL OF MICROWAVE AND OPTICAL TECHNOLOGY

VOL. 3, NO. 3, JULY 2008

Study and Fabrication of Metamaterials for Electronics and Telecommunications Applications

A. Andreone[*], F. Frezza[**], V. Galdi[***], A. Scaglione[****], and L. Vegni[*****]
[*]Department of Physical Sciences, University of Naples "Federico II", Naples, ITALY
Tel: +39-081-7682-547; Fax: +39-081-2391-827; E-mail: antonello.andreone@unina.it
[**]Department of Electronics Engineering, University of Roma "La Sapienza", Rome, ITALY
Tel: +39-06-4458-5841; Fax: +39-06-4742-647; E-mail: fabrizio.frezza@uniroma1.it
[***]Department of Engineering, University of Sannio, Benevento, ITALY
Tel: +39-0824-305809, Fax: +39-0824-305840; E-mail: vgaldi@unisannio.it
[****]DIIIE, University of Salerno, Salerno, ITALY
Tel: +39-089-96-4249; Fax: +39-089-96-4176; E-mail: ascaglione@unisa.it
[*****]Department of Applied Electronics, University of Roma Tre, Rome, ITALY
Tel: +39-06-5733-7003; Fax: +39-06-5733-7026; E-mail: vegni@uniroma3.it

***Abstract*- The research activities developed by five Italian academic partners (Universities of Roma Tre and "La Sapienza", Sannio, Salerno, and Naples "Federico II") in the frame of a PRIN 2006 research project, supported by the "Ministero dell'Università e della Ricerca," are presented. The project involves theoretical investigation, numerical analysis, fabrication, and experimental characterization of metamaterials and (quasi-) periodic structures for applications in electronic devices and telecommunication systems. After a brief introduction about the main goals of the project, the scientific results achieved by the different research units will be detailed.**

***Index Terms*- Metamaterials, complex materials, (quasi-)periodic structures, miniaturization, superlenses, leaky-wave antennas, fractal dielectric multilayers.**

I. INTRODUCTION

The PRIN 2006 research project entitled "*Study and fabrication of metamaterials for electronics and telecommunications applications*" brings together the research expertises and the facilities of five academic partners in order to conceive, design and fabricate innovative microwave components based on different kinds of *metamaterials*.

These materials exhibit unusual properties not readily available in natural materials. Such properties pave the way to revolutionary breakthroughs for the electronic and telecommunication industry, such as even more miniaturized components, multi-functional and super-directive radiators, imaging systems with unconventional resolution, high-Q cavities and resonators, ultra-compact filters, ultra-fast switches, low-power micro-lasers, systems for ultra-fast optical computation, etc.

The research activities developed in the project focus mainly on the microwave applications of different classes of metamaterials, including negative refractive index or Double NeGative (DNG) materials, materials characterized by a negative permittivity or permeability, Electromagnetic Band-Gap (EBG) materials, materials made of printed periodic structures, etc...).

In this frame, the goal is to propose theoretical models for analysis, numerical methods for simulation and optimization, fabrication and measurement techniques for appropriate experimental characterization of different components, such as miniaturized antennas and absorbers, superlensing devices, highly-directive antennas, directional couplers with high coupling values, etc...

II. SUMMARY OF MAIN ACTIVITIES AND RESULTS

A. *Miniaturized components and EBG-based radiators* (University of Roma Tre)

One of the goals of the project is to demonstrate miniaturized radiators made by pairing together metamaterials with opposite values of the constitutive parameters [1-4].

Circular patch antennas with dimensions less than 1/20 of the operating wavelength have been demonstrated through extensive numerical simulations and experimental data.

As an example, in Fig.1a) the current density distribution at the resonant frequency 0.48 GHz when the circular patch antenna is loaded with Split Rings is depicted. The result is in good agreement with the one in the case of an ideal Mu NeGative (MNG) core. The desired mode, thus, has been effectively excited in a sub-wavelength radiating structure loaded with Split Rings. In Fig.1b) the return loss as a function of the frequency and the radiation pattern at the two resonant frequencies are shown. The gain at the lower frequency is much smaller than the one at the highest frequency. Nevertheless, considering the electrically small dimensions of the antenna at the lower operating frequencies, this result can be considered as rather promising.

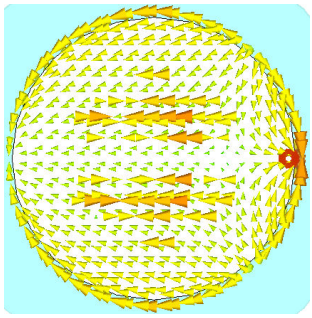

Fig.1a) current density distribution at the resonant frequency 0.48 GHz of a circular patch antenna loaded with Split Rings.

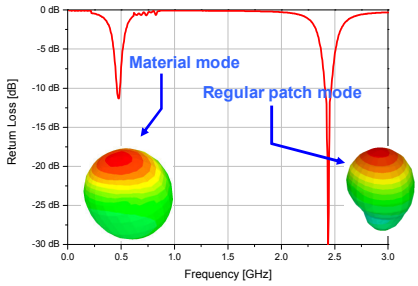

Fig.1b) Return Loss as a function of the frequency and 3D gain pattern of the antenna at the two resonant frequencies.

Resonant microwave absorbers with dimensions smaller than 1/100 of the free-space wavelength have also been designed and their experimental characterization is under progress.

The theoretical formulation of the problem is based on the equivalent transmission line network representation of the absorber and on the assumption that metamaterials may be represented as isotropic media described by simple dispersion models.

This theoretical approach is validated through a full-wave numerical analysis, confirming the effectiveness of the absorber in terms of size reduction.

This analysis gives some interesting physical insights into the operation mechanism of the component. Some applications of the designed absorbers in the field of antennas and radar-absorbing materials have been studied under the assumption that ideal metamaterials are replaced by real-life inclusion-made materials.

The design is conducted in order to have the desired bandwidth and isotropy properties. Some absorber samples are being realized and characterized in cooperation with industrial partners (Fig.2). Practical artificial materials with magnetic properties and metamaterials with anomalous values of the permeability are of interest for several applications in different frequency ranges and can be obtained via Split Ring Resonators (SRRs) inclusions. SRRs have been firstly introduced to demonstrate materials with a negative permeability at microwaves.

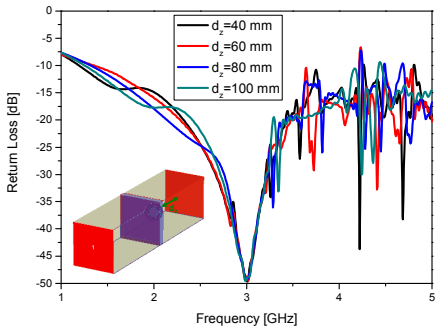

Fig.2 Return Loss proper of metallic sphere behind the planar absorber.

They have been usually used in the early applications of metamaterials to design magneto-dielectrics, MNG and Mu Near Zero (MNZ) materials. However, their dimensions are usually of the order of $\lambda/20$ and, thus, when going from the first demonstration of the material properties towards the actual fabrication of working miniaturized components, this limitation may become a deep barrier.

A basic idea to overcome this limitation and to reduce the dimensions of the resonant inclusions is to use Multiple Split-Ring Resonators (MSRRs) (Fig.3) or Spiral Resonator (SRs) (Fig.4) which increase the distributed capacitance between the strips without increasing the area occupied by the resonator.

Two different circuit models of MSRR and SR in presence of air and ideal conductors have been studied. Such circuit representations overcome the limits of the models previously available in the open technical literature and are able to give more accurate results if compared to full-wave numerical simulations.

On the other hand, when moving toward higher frequencies, miniaturization might not be an issue any more. Sometimes, indeed, miniaturization is to avoid, due to the technological limitations to print sufficiently small inclusions. In this case, the design strategy is different and new concepts, other than the ones used to design MSRRs and SRs, have to be employed. In this frame, SRs are able to alleviate and/or overcome this limitation.

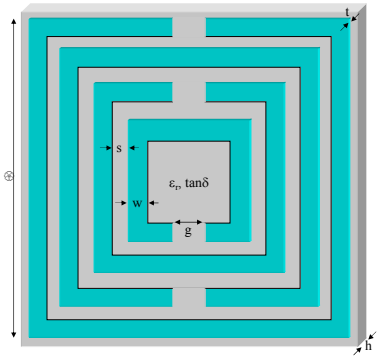

Fig.3 Sketch and geometrical dimensions of a MSRR.

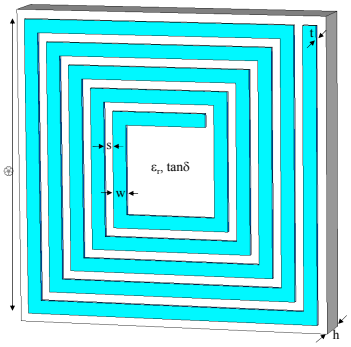

Fig.4 Sketch and geometrical dimensions of a SR.

To overcome the limitation in the coupling values achievable in regular coupled microstriplines, a layout has been studied (Fig.5).

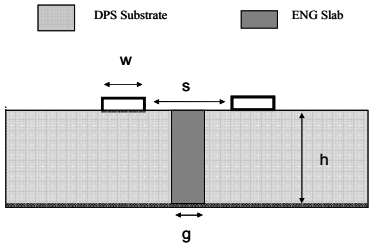

Fig.5 Coupled microstriplines with an ENG slab inside the substrate.

An isotropic and homogeneous Epsilon NeGative (ENG) thin slab is placed between the two strips inside the homogeneous and isotropic dielectric substrate. In the frequency band of operation, the metamaterial slab exhibits negative values of the real part of the permittivity, while the substrate is assumed to be

made by a high-index material (i.e. alumina). The negative permittivity of the ENG slab is assumed to be, as absolute value, much smaller than the substrate permittivity.

As an example, a power divider (i.e. a -3dB coupling value) has been designed. The ENG slab was an isotropic material described through the Drude dispersion law, with the plasma frequency at 1.4 GHz. This material exhibits the needed value of the relative permittivity equal to -0.70 at the frequency 1.035 GHz. Full-wave numerical simulations confirm the expected behavior. Results of Fig.6 can be compared with those of Fig.7, where the amplitude of the scattering parameters are reported when the ENG slab is removed. From this comparison, it is clear that the introduction of the ENG slab gives a coupling value not obtainable in standard conditions.

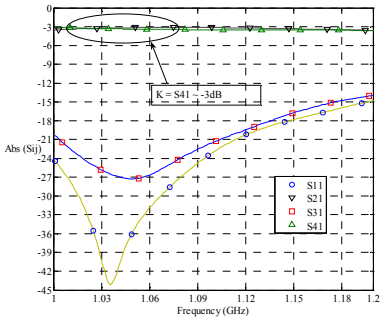

Fig.6 Amplitude of the scattering parameters.

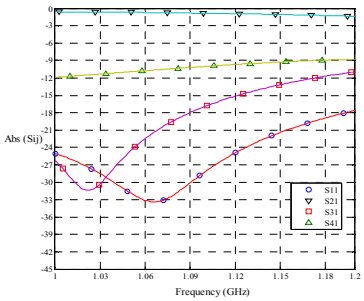

Fig.7 Scattering parameters of the coupler without the ENG slab.

Finally, in the frame of the activities on radiating systems, new techniques have been developed for the design of 3D EBGs with defects which can be very useful to realize directive planar antennas. Reflection and transmission properties of such media were studied by using a Fourier Modal-Method (FMM). An EBG is actually a stack of binary gratings separated by homogeneous layers (see [5], where an accurate, versatile, and fast modeling of two-dimensional (2D) electromagnetic crystals is presented). Analogously, a finite-thickness 3D-EBG (i.e., infinitely extending only in two directions) can be considered as a superposition of doubly-periodic gratings. For the scattered field in the homogeneous regions, use is made of Rayleigh expansions; inside the periodic region, and modal expansions of the field components are employed. Fig.8 shows a comparison with results available in the literature, for a checkerboard structure, Fig.8(a), with normally-incident illumination, polarization along x axis.

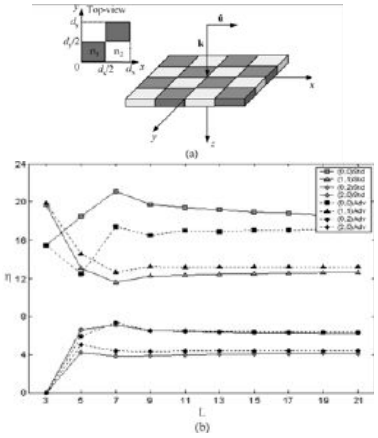

Fig.8(a) Checkerboard structure. (b) Comparison with the literature. Markers: obtained results; full and dotted lines: results reported by Li [6].

Fig.8(b) presents the transmission efficiency of (0,0), (1,1), (0,2), and (2,0) orders as a function of the number of diffracted orders considered in each periodic direction. It can be seen that the agreement with the results in [6] is very good. Both the standard eigenvalue solution and the advanced one, in which a better treatment of the discontinuities of the functions is carried out, are considered: it can be appreciated that the convergence of the advanced method is faster.

B. *Microstrip metamaterial leaky-wave antennas* (University of Roma "La Sapienza")

Leaky-wave antennas (LWAs) realized through one-dimensional periodic microstrip lines are attractive structures, which have been studied in this research project. Their main feature is to provide a simple means of obtaining a narrow fan beam that scans with frequency. These antennas are versatile and easy to fabricate, since they consist of a purely-planar metallic structure that is periodically modulated along its length.

The introduction of the periodic perturbation produces an infinity of space harmonics, some of which may be fast while the rest are slow; the fast space harmonics radiate. Since one usually desires an antenna that radiates only a single beam, the structure is designed so that only one space harmonic is fast. As a result, these periodic structures guide a leaky mode that propagates along their length, with radiation occurring from the single space harmonic that is fast. Conventional LWAs radiate through the n=−1 space harmonic; however, with the emerging trend of metamaterials, a new kind of LWAs has been recently proposed, which has the fundamental n=0 harmonic fast. Such antennas may be considered quasi-uniform LWAs due to their effectively uniform nature, even though they are structurally periodic [7], [8]. The periodicity allows for a frequency scannable beam that can scan from the backward to the forward quadrant, but it is well known that a scan angle at broadside corresponds to an "open stopband." Near the open stopband frequency, the attenuation constant of the leaky mode typically changes quite rapidly, and often drops to zero.

This results in undesirable scan performances near broadside with a beam that cannot be pointed at broadside in the presence of a unidirectional source [9]-[11].

A design example of a microstrip metamaterial leaky-wave antenna optimized for broadside scanning is reported in Fig.9.

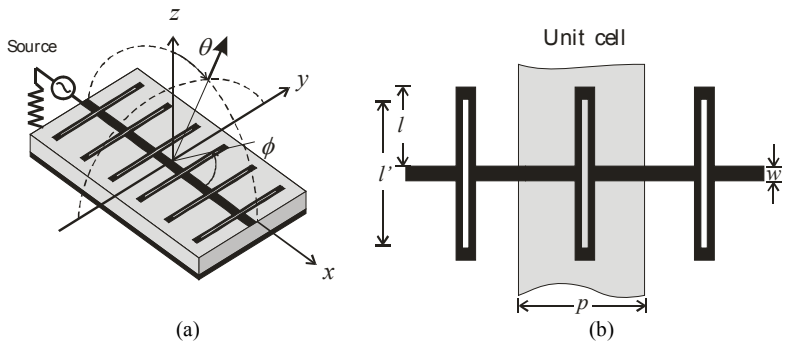

Fig.9. Periodic leaky-wave antenna with a unidirectional source (p=4 mm, w=0.6 mm) printed on a substrate with height h=0.767 mm, and dielectric constant ε_r=10.2. The discontinuity within the unit cell is characterized by l=4 mm and l'= 7.4 mm. (a) 3D view. (b) Top view.

The relevant normalized phase and attenuation constants are reported in Fig.10a for the n=−1 harmonic. These results are obtained by means of a periodic full-wave method of moment approach [12]. It can be noticed that the phase constant passes continuously from negative values to positive values as the frequency increases [11], [12]. This implies a continuous scanning from the backward to the forward quadrant. Moreover, the attenuation constant remains almost constant in the scanning frequency range, thus allowing for a constant beamwidth and an equalized radiation efficiency [9]-[11].

To prove the effectiveness of the design, a finite structure (48 cells) excited by a gap source has been simulated with Ansoft Designer™.

In Fig.10b the gain as a function of the scanning angle is reported for three different frequencies showing the continuous scanning capability.

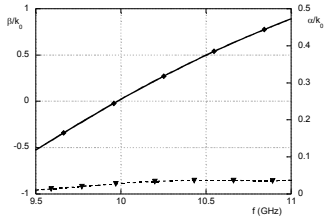

Fig.10a Phase (solid line) and attenuation (dashed line) constants normalized to the free-space wavelength as a function of frequency for the n=−1 harmonic.

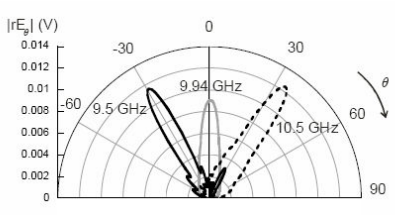

Fig.10b Gain as a function of the scan angle θ in the ϕ=0° plane for three frequencies: 9.5 GHz, 9.94 GHz, 10.5 GHz.

In Fig.11 normalized radiation patterns are reported for the same frequencies in order to show the almost constant beamwidth at -3 dB.

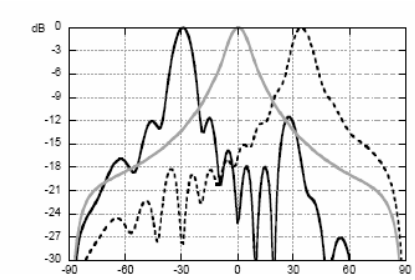

Fig.11 Radiation patterns n as a function of the scan angle θ in the ϕ=0° plane for three frequencies: 9.5 GHz, 9.94 GHz, 10.5 GHz.

C. *Photonic crystals and photonic quasicrystals* (University of Naples "Federico II" and University of Sannio)

Photonic crystals

Photonic crystals (PCs) are artificial periodic structures reproducing natural crystals at different length scale. PCs can control and manipulate the flow of light in many different ways. Amongst a variety of recently discovered dispersion phenomena, including superprism and negative refraction effects, focus here is on the experimental observation of the Pendellösung effect in PCs. Since the original formulation of the diffraction theory from Ewald [13], this effect was predicted in perfect crystals as a periodic exchange of energy between interfering wave-fields [14].

The Pendellösung effect in PCs can be understood as a beating phenomenon due to the phase modulation between coexisting plane wave components, propagating in the same direction. The coexistence is possible because such wavevectors are associated to two adjacent bands that are overlapped, for a given frequency, in correspondence of suitably chosen PC parameters. A 2D periodic structure consisting of dielectric rods in air, (dielectric permittivity ε_r=8.6) arranged in a square geometry and having r/a=0.255, where r is the cylinder radius and a is the lattice constant, has been studied. If *TE* polarization (electric field parallel to the rods axis) is considered, an overlap occurs between the forth and the fifth mode for a normalized frequency $f_n=a/\lambda$ = 0.722 (with λ denoting the free-space wavelength). As a consequence of the Pendellösung effect, the intensity I at the exit surface is harmonically modulated as a function of the thickness t [14]. When t is an even multiple of half the Pendellösung distance Λ_0, the beam at the exit surface is parallel to the incident beam, forming a positive angle with respect to the PC normal. On the other hand, when t is an odd multiple of Λ_0 the beam at the exit surface is completely directed along the Bragg diffracted direction, forming a negative angle with respect to the PC normal.

Measurements are carried out by placing alumina rods with nominal permittivity ε_r=8.6, radius r=0.4 *cm* and height h=1 *cm* in a square geometry with r/a=0.255 (a=1.57 *cm*) sandwiched in an aluminium parallel-plate waveguide terminated with microwave absorbers. Using these parameters the Pendellösung distance turns out to be $\Lambda_0=4a$.

The microwave PC is built in the shape of a 38.5 *cm* wide slab (25 rod columns), with a thickness

that can be varied adding or removing rows. A dipole antenna is used as source, oriented to produce an electric field parallel to the rods axis and operating at the frequency of 13.784 *GHz*, in order to reproduce the same normalized frequency a/λ of the theoretical model. The spatial distribution of the electromagnetic wave transmitted by the 2D PC having a different number of rows (different thickness) is measured at the exit surface, by using a HP8720C Vector Network Analyzer and another dipole antenna as a detector, that moves along the waveguide plane using an *x-y* step motor. The analysis was focused on structures with a number of rows *n* ranging from 1 to 10.

In Figs.12(a)-(e) the real part of the electric field experimentally detected in different crystal configurations is mapped in the image plane, using a normalized scale. In Fig.12(a) the spatial distribution is shown for the case n=10. The maps for the other cases of crystals with an even number of rows (n=8,6,4,2) are presented in Figs.12(b), (c), (d), (e), respectively.

Starting the data analysis from the PC consisting of ten rows, that is an odd multiple of $\Lambda_0/2$, in this case the beam, as expected, is fully transmitted in the diffracted direction. On the contrary, when the PC consists of 8 rows, the beam exits its surface in the forward diffracted direction (Fig.12(b)). By reducing the thickness down to two rows for any even *n*, the transmitted beam alternatively bends from the negative to the positive direction, as shown in Figs.12(c)-(e). Measurements clearly show therefore that for an even number of rows the involved energy is almost entirely concentrated along one exit direction only. On the contrary, for an odd number of rows, according to the periodical modulation predicted for the field intensity at the exit surface, the thickness is such that at the crystal-air interface the transmitted energy is equally divided in both positive and negative directions.

This is shown in Figs.12(f)-(j): the electromagnetic beam in the image plane actually splits in two beams having approximately the same intensity, with equi-phase planes clearly evident in both directions. It is worth noting that the case with n=1 (Fig.12(j)) reduces to the well known Bragg grating.

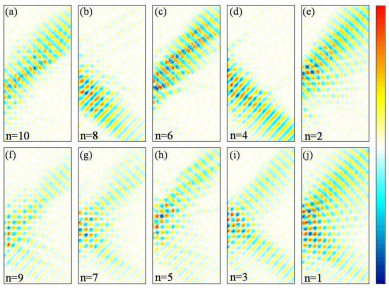

Fig.12 (color online) Mapping of the measured electric field (real part) in a normalized scale for: (a)-(e) even *n*; (f)-(j) odd *n*.

Photonic quasicrystals

During the last decade, photonic quasicrystals (PQCs), composed of metallic or dielectric inclusions arranged according to "*aperiodic tilings*" [15] emerged as interesting alternatives to standard periodic PC configurations in a variety of applications (see [16] for a recent review of the subject).

In what follows, some numerical and experimental results concerning directive emission and focusing are summarized.

Directive Emission

Following up on some preliminary studies, 2D PQC slabs are here considered (Fig.13) made of infinite dielectric rods arranged according to three representative categories of aperiodic tilings (Penrose [15], octagonal [16], dodecagonal [17]), (Fig.14).
From suitably large tilings, the PQC slabs were generated by cutting (symmetrically around the local center of symmetry) rectangular portions of size $L \times h$, and placing at the tile vertices (in free space) circular dielectric rods of relative permittivity $\varepsilon_r = 12$ and radius $r = 0.138a$, with a being the lattice constant (tile sidelength).
In all simulations below, the structures are assumed to have same lattice constant and comparable size and filling factor, to be defect-

free, and to be excited by a time-harmonic electrical line-source located nearby the slab center.

Via a comprehensive parametric study carried out using a well-established full-wave technique based on a multipolar Fourier-Bessel expansion [18], directive broadside radiation with moderate to low sidelobe level (SLL) at several frequencies was observed.

For the sake of space, Table 1 summarizes some representative configurations yielding reasonably good tradeoff performances, in terms of normalized operational frequency a/λ, broadside directivity D, broadside radiated intensity S (normalized to its free-space value), and SLL.

As an example, Fig.15 shows the best radiation pattern observed in this study, corresponding to a dodecagonal PQC.

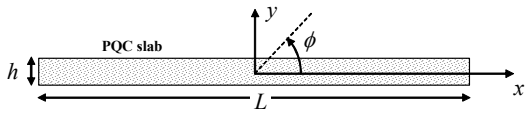

Fig.13 Problem geometry (details explained in the text).

To sum up, this study evidences, for the first time in the literature, the possibility of achieving directive low-sidelobe emission, at multiple frequencies, from defect-free PQC slabs.

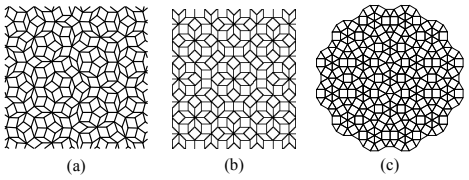

Fig.14 Samples of the "*thick-and-thin*" Penrose (a), octagonal (b), and dodecagonal (c) tilings.

Current and future studies are aimed at a deeper understanding of the underlying phenomena, including the role of (local vs. global) order and symmetry, as well as the development of semi-analytic (leaky-wave) parameterizations of the radiated field.

Table 1: Summary of representative parametric configurations yielding good tradeoff performances.

Type	a/λ	D [dB]	S [dB]	SLL [dB]
Penrose	0.310	9.40	6.25	-5.68
Octagonal	0.258	11.15	11.58	-6.44
Dodecagonal	0.239	15.5	14.8	-11.9

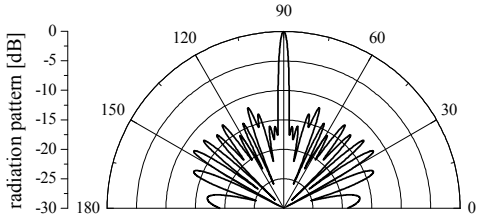

Fig.15 Radiation pattern for a dodecagonal PQC slab with L=97.8a, h=4a (435 rods), with source at x_s=0, y_s=1.55a, at normalized frequency $a/\lambda = 0.239$.

Focusing

Numerical and experimental observations of negative refraction and "*superlensing*" in a dodecagonal PQC structure appeared in literature only recently [19]. However, a clear interpretation of such properties, as well as a full understanding of the underlying mechanisms, is still lacking. To clarify at least some of the above aspects, a comprehensive parametric study was carried out using the aforementioned multipolar Fourier-Bessel expansion [18], backed by experimental microwave measurements. A dodecagonal PQC (Fig.14(c)), was considered with $\varepsilon_r = 8.6$ and r=0.4 cm, and lattice constant a=4⁄3 cm. A flat-lens prototype was fabricated by placing alumina rods in the previously described parallel-plate-waveguide measurement setup, using a monopole antenna as a microwave source to produce an electric field parallel to the rods axis. Fig.16 shows a numerically-computed intensity map which illustrates the focusing properties of this structure, reproducing the results in [19].

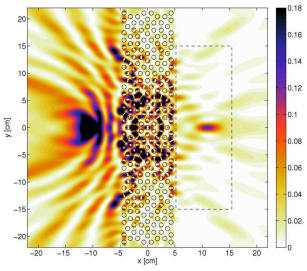

Fig.16 (color online) Simulated field intensity map at 8.836 GHz for a dodecagonal PQC slab (L=42.9 cm, h=9.4 cm), illustrating the focusing of a source placed at y_s=0 and at a distance d_x=6 cm from the slab surface. The dashed rectangle delimits the 10 cm×30 cm area scanned in the image-side measurements.

Fig.17 shows some representative measured and simulated field intensity maps at the image side of the PQC slab, for orthogonal and parallel (to the slab interface) displacements of the source. A general good agreement is observed between simulations and measurements.

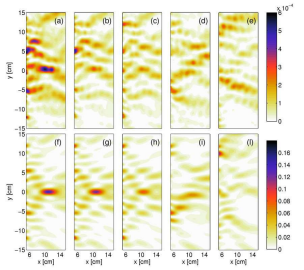

Fig.17 (color online) As in Fig.16, but details of the measured (a–e) and simulated (f–l) field intensity maps at the image side, for various source positions. (a), (f): Source at y_s=0, and at a distance d_x=6 cm from the slab surface; (b), (g): y_s=0 and d_x=7 cm; (c), (h): y_s=0 and d_x=8 cm; (d), (i): y_s=1cm and d_x=6 cm; (e), (l): y_s=5 cm and d_x=6 cm.

For orthogonal displacements, the focus image positions do not seem to follow the ray model predicted for flat lenses with *n=-1*. For small parallel displacements, moving the source away from the central position produces images with a distorted focus, that abruptly disappears when increasing the displacement. To sum up, this numerical and experimental study of the focusing properties of dodecagonal PQCs confirms some of the results reported in the recent literature [19], but shows that, contrary to the original interpretation, such results are not attributable to an "*effective negative refractive-index.*" Instead, they seem to arise from complex near-field scattering effects and short-range interactions critically associated to local symmetry points in the PQC, which deserve deeper investigations.

D. *Aperiodic one-dimensional EBG structures: fractal dielectric multilayer* (University of Salerno)

EBG structures can be realized as layered dielectric structures either periodic or nonperiodic.

Among the various types of nonperiodic structures, the ones characterized by fractal morphology show attractive features for devices in both optical and microwave frequency bands (frequency selective surfaces, filters, sensors, etc…). Fractals are self-similar structures characterized by invariance property with respect to a change of scale. They can be constructed by starting from a basic element and repeating a particular operation on smaller and smaller scales [20]. A triadic Cantor fractal multilayer is a layered structure in which the sequence of the thicknesses of the layers reproduces a triadic Cantor set (Fig.18a).

In this case, the constructing procedure consists in replacing the 3-rd middle part of a dielectric layer of relative permittivity ε_a and thickness Δ with a dielectric of relative permittivity ε_b and repeating such a substitution on all the obtained layers of permittivity ε_a. A triadic optical Cantor multilayer (TOCM) can be constructed by enforcing the Cantor construction rule to the optical thicknesses of the constituent layers [21]. In this case the optical thickness of the overall structure does not depend on the stage of growth of the fractal, i.e. on the number of steps of the substitutional procedure.

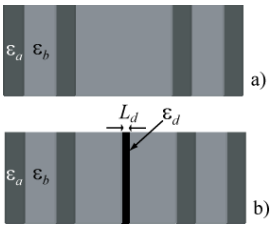

Fig.18a) Triadic Cantor fractal multilayer at the 3-rd stage of growth; b) Perturbed multilayer.

The transmission spectrum of a TOCM exhibits a deep stop-band (centered at the frequency at which the thinnest layers are quarter-wavelength optically thick) in which two very narrow transmission peaks appear. Compared to the transmission peak (defect mode) that originates in the band-gap of a periodic structure perturbed by a defect layer (i.e. a dielectric layer with permittivity $\varepsilon_d \neq \varepsilon_a, \varepsilon_b$), the peaks of the TOCM are considerably narrower and have a larger quality factor $Q=f_c/\Delta f$ (f_c and Δf being the central frequency and the -3 dB bandwidth of the peak, respectively). Fig.19 shows one of the two transmission peaks bounding the band-gap of a TOCM (ε_a=4.7 and ε_b=2.1) at the 4-th stage of growth (31 layers) having the thinnest layers 377-nm optically thick. The structure response was calculated for normal incidence by using the conventional transmission matrix method and assuming the medium bounding the multilayer to be air. Also plotted in the figure is the defect mode of a periodic multilayer with 32 377-nm optically thick layers of the same constituent materials, perturbed by a central defect layer (ε_d=6.25, optical thickness 377 nm). As can be seen, the transmission peak of the TOCM is narrower than the one of the periodic structure and exhibits a larger quality factor (6169.6 vs. 1408.7). Perturbing the fractal morphology by inserting a defect layer (Fig.18b) causes a shift of the transmission peaks bounding the structure band-gap toward lower frequencies. The size of this shift depends on either the permittivity ε_d or the thickness L_d of the defect layer and can cover the overall band-gap. Fig.20 shows the frequency shift of the transmission peak of the TOCM perturbed by a layer with ε_d=6.25 and L_d= 194 nm.

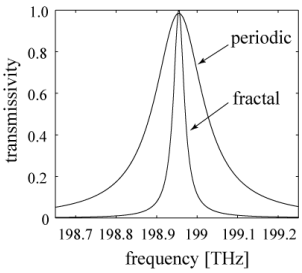

Fig.19 Transmissivity peaks of the two analyzed multilayer structures.

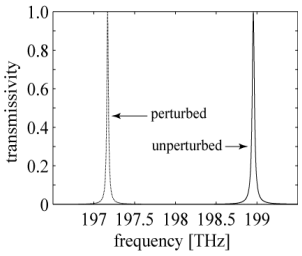

Fig.20 Effect of a perturbing defect layer on the transmissivity spectrum of the triadic Cantor fractal multilayer.

Finally, the influence of material absorption on the filtering performance of the fractal multilayer was also investigated and the resulting passband characteristics were compared to the ones of a lossy periodic multilayer. When all constituent dielectrics are lossy, both structures retain the same filtering performance as the losses increase. When losses affect only one of the two constituent dielectrics (the one with the largest permittivity), Cantor multilayers exhibit better filtering performance. This is illustrated in Fig.21 where the quality factor is plotted as a function of the loss tangent of the dielectric with permittivity ε_a for structures having the same Q in the lossless case (to this end the periodic multilayer must have 40 layers). As can be seen, the quality factor of the TOCM keeps always noticeably higher than the one of the perturbed periodic multilayer.

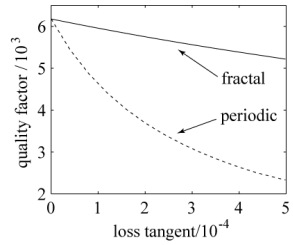

Fig.21 Quality factor of the transmissivity peak of lossy multilayer structures.

To sum up, it has been shown that the fractal Cantor morphology allows to design dielectric multilayers having passband filtering responses with quality factors remarkably higher than the perturbed periodic one. Perturbing the fractal multilayer by inserting a defect layer, causes the

transmission spectrum to shift toward lower frequencies thus allowing a very narrow band tunable filter to be designed. Moreover, the fractal morphology can be particularly beneficial in the presence of material absorption.

CONCLUSIONS

In this paper, the research activities developed within the frame of the PRIN 2006 project entitled "*Study and fabrication of metamaterials for electronics and telecommunications applications*" have been summarized with particular enphasis on the novel results obtained.

REFERENCES

[1] A. Alù, F. Bilotti, N. Engheta, and L. Vegni, "Sub-wavelength, compact, resonant patch antennas loaded with metamaterials," *IEEE Trans. Antennas Propagat.*, Vol. 55, pp. 13-25, Jan. 2007.

[2] F. Bilotti, A. Alù, N. Engheta, and L. Vegni, "Miniaturized circular patch antenna with metamaterial loading," Proc. EuCAP 2006, Nice, France, 6-10 Nov., 2006.

[3] F. Bilotti, S. E. Lauro, A. Toscano, and L. Vegni, "Efficient modeling of the crosstalk between two coupled microstrip lines over non conventional materials using an hybrid technique," accepted for publication in *IEEE Transactions on Magnetics*.

[4] A. Toscano, L. Vegni, F. Bilotti, and S. E. Lauro, "Metamaterials as complex dielectrics in the design of a new class of integrated circuits," Proc. SPIE Europe's International Congress on Optics & Optoelectronics (ICOO), Prague, Czech Republic, 16-19 Apr., 2007

[5] F. Frezza, L. Pajewski, and G. Schettini, "Characterization and design of two-dimensional electromagnetic bandgap structures by use of a full-wave method for diffraction gratings," *IEEE Trans. Microw. Theory Tech.*, Vol. 51, pp. 941-951, Mar. 2003.

[6] L. Li, "New formulation of the Fourier modal method for crossed surface-relief gratings," *J. Opt. Soc. Amer. A*, Vol. 14, pp. 2758-2767, Oct. 1997

[7] C. Caloz, T. Itoh, *Electromagnetic Metamaterials: Transmission Line Theory and Microwave Applications. The Engineering Approach*, Hoboken, NJ, John Wiley & Sons, Inc., 2006.

[8] S. Paulotto, P. Baccarelli, F. Frezza, and D. R. Jackson, "Full-wave analysis and broadside optimization for the microstrip CRLH leaky-wave antenna," Proc. *Metamaterials 2007*, Rome, Italy, Oct. 2007, pp. 489-492.

[9] P. Baccarelli, S. Paulotto, and D. R. Jackson, "Broadside radiation properties of 1D microstrip leaky-wave antennas," *Proc. ICEAA'05*, Torino, Italy, 12-16 Sept. 2005, pp. 755–758.

[10] S. Paulotto, P. Baccarelli, F. Frezza, and D. R. Jackson, "A novel technique to eliminate the open stopband in 1-D periodic printed leaky-wave antennas," Proc. *EuCAP 2007*, Edinburgh, Scotland, Oct. 2007.

[11] S. Paulotto, P. Baccarelli, F. Frezza, and D.R. Jackson, "A microstrip periodic leaky-wave antenna optimized for broadside scanning," Proc. 2007 IEEE Antennas Propagat. International Symp., Honolulu, HI, USA, 9-15 June 2007, pp. 5789-5792.

[12] P. Baccarelli, C. Di Nallo, S. Paulotto, and D. R. Jackson, "A full-wave numerical approach for modal analysis of 1D periodic microstrip structures," *IEEE Trans. Microw. Theory Tech.*, Vol. 54, pp.1350-1362, Apr. 2006.

[13] P.P. Ewald, "Zur Theorie der Interferenzen der Röntgenstrahlen," *Physik Z.*, Vol. 14, pp. 465-472, 1913.

[14] V. Mocella, "Negative refraction in photonic crystals: thickness dependence and Pendellösung phenomenon," *Opt. Express*, Vol. 13, pp. 1361-1367, Mar. 2005.

[15] M. Senechal, *Quasicrystals and Geometry*, Cambridge University Press, Cambridge, UK, 1995.

[16] W. Steurer and D. Sutter-Widmer, "Photonic and phononic quasicrystals," *J. Phys. D: Appl. Phys.*, Vol. 40, pp. R229-R247, July 2007.

[17] M. Oxborrow and C.L. Henley, "Random square-triangle tilings: A model for twelvefold-symmetric quasicrystals," *Phys. Rev. B*, Vol. 48, pp. 6966-6998, Sep. 1993.

[18] D. Felbacq, G. Tayeb, and D. Maystre, "Scattering by a random set of parallel cylinders," *J. Opt. Soc. Am. A*, Vol. 11, pp. 2526-2538, Sep. 1994.

[19] Z. Feng, X. Zhang, Y. Wang, Z.-Y. Li, B. Cheng, and D.-Z. Zhang, "Negative refraction and imaging using 12-fold-symmetry quasicrystals," *Phys. Rev. Lett.*, Vol. 94, 247402, June 2005.

[20] X. Sun and D.L. Jaggard, "Wave interactions with generalized Cantor bar fractal multilayers", *J. Appl. Phys.*, Vol. 70, pp. 2500-2507, 1991.

[21] F.Chiadini, V.Fiumara, I.M. Pinto, and A.Scaglione, "Self-scaling properties of the reflection coefficient of Cantor prefractal multilayers," *Microw. Opt. Technol. Lett.*, Vol. 37, pp. 339-343, 2003.